Anomalous collisional absorption of laser pulses in underdense plasma at low temperature

M. Kundu
Institute for Plasma Research, Bhat, Gandhinagar, Gujarat 382 428, India
(Received 3 November 2014; published 6 April 2015)

In a previous paper [M. Kundu, Phys. Plasmas **21**, 013302 (2014)], fractional collisional absorption (α) of laser light in underdense plasma was studied by using a classical scattering model of electron-ion collision frequency ν_{ei}, where total velocity $v = \sqrt{v_{th}^2 + v_0^2}$ (with v_{th} and v_0 as the thermal and the ponderomotive velocity of an electron) dependent Coulomb logarithm $\ln\Lambda(v)$ was shown to be responsible for the anomalous (unconventional) increase of ν_{ei} and α ($\propto\nu_{ei}$) with the laser intensity I_0 up to a maximum value about an intensity I_c in the low temperature ($T_e < 15$ eV) regime and a conventional $\approx I_0^{-3/2}$ decrease when $I_0 \gg I_c$. One may object that the anomalous increase in ν_{ei} and α were partly due to the artifact introduced in $\ln\Lambda$ through the maximum cutoff distance $b_{max} \propto v$. In this work, we show similar anomalous increase in ν_{ei} and α versus I_0 (in the low temperature and underdense density regime) with more accurate quantum and classical kinetic models of ν_{ei} without using $\ln\Lambda$, but with a proper choice of the total velocity dependent inverse cutoff length $k_{max} \propto v^2$ (classical) or $k_{max} \propto v$ (quantum). For a given $I_0 < 5 \times 10^{14}$ W cm^{-2}, ν_{ei} versus T_e also exhibits so far unnoticed identical anomalous increase as ν_{ei} versus I_0, *even* if the conventional $k_{max} \propto v_{th}^2$ or $k_{max} \propto v_{th}$ (without v_0) is chosen. The total velocity dependent k_{max} in the kinetic models, as proposed here, is found to explain the anomalous increase of α with I_0 measured in some earlier laser-plasma experiments.

DOI: 10.1103/PhysRevE.91.043102 PACS number(s): 52.50.Jm

I. INTRODUCTION

Absorption of laser light in dense plasma occurs via (i) collisionless and (ii) collisional processes. There are a plethora of collisionless mechanisms, e.g., linear resonance [1–5], anharmonic resonance [6–11], Brunel heating [3,4,12], etc., which happen only by meeting specific conditions between laser and plasma parameters. However, collisional absorption [1–4,13–20] through electron-ion collision (inverse bremsstrahlung) occurs almost all the time in the subrelativistic laser field. Although more than three decades have been spent in the understanding of collisional absorption in laser-driven plasmas, there is no universal agreement in the literature for the average electron-ion collision frequency (ν_{ei}) in the laser field [1,2,21–26]. In the classical scattering model (CSM) of ν_{ei} (based on the Rutherford scattering), this disagreement is due to the lack of knowledge of the exact form of the Coulomb logarithm ($\ln\Lambda$) in the expression of ν_{ei}, where $\ln\Lambda$ depends on the maximum and minimum cutoff distances (b_{max} and b_{min}) of an electron from a colliding ion through the relation $\ln\Lambda = 0.5\ln(1 + b_{max}^2/b_{min}^2)$. However, the dependence of b_{max} and b_{min} on the laser and plasma parameters is still a debatable issue [23–25,27–29], which makes ν_{ei} uncertain. Unless explicitly noted, for our convenience we use atomic units (a.u.) through out this paper, i.e., $|e| = m_e = \hbar = 4\pi\epsilon_0 = 1$, where e and m_e are charge and mass of an electron, $\hbar$ is the reduced Planck constant, and ϵ_0 is the permittivity of the free space.

In the case of an overdense plasma (where plasma frequency $\omega_p = \sqrt{4\pi n_p}$ is higher than the laser frequency ω), the maximum cutoff b_{max} is conventionally taken as the Debye screening length $\lambda_d = v_{th}/\omega_p$. Here $v_{th} = \sqrt{T_e}$ is the electron thermal velocity, T_e is the plasma temperature, and $n_p = n_e = Zn_i$ is the plasma density, where n_e,n_i are electron and ion density, and Z is the ionic charge state. For the underdense plasma ($\omega_p < \omega$) there should be either no screening or it should be reduced. Based on this argument, $b_{max} = v_{th}/\omega$ is chosen (in the underdense case) in many earlier works [1,2,21,22,26,30,31]. Classically, b_{min} is obtained by balancing the Coulomb potential energy $Ze^2/4\pi\epsilon_0 b_{min}$ with the thermal energy eT_e of an electron, which gives the conventional $b_{min} = Z/v_{th}^2$ (in a.u.). On the other hand, when quantum phenomena are important, b_{min} is taken as the thermal DeBroglie wavelength, i.e., $b_{min} = \lambda_B = (2v_{th})^{-1}$. Thus, in either case, $\ln\Lambda$ is conventionally taken to be independent of the ponderomotive velocity $v_0 = E_0/\omega$ and the field strength E_0. As a consequence, for a given n_p, T_e, and ω, one finds that ν_{ei} initially remains almost constant [22,26,32–34] with increasing v_0/v_{th} up to some value of v_0/v_{th}, then decreases as v_0^{-3} when $v_0/v_{th} \gg 1$ (see Fig. 1 in Ref. [22]). In terms of the laser intensity $I_0 \propto v_0^2$, ν_{ei} remains constant up to some intensity I_c, then it decreases as $I_0^{-3/2}$ when $I_0 \gg I_c$. The corresponding fractional absorption α (defined as the ratio of the absorbed laser energy to the incident laser energy) of the laser pulse vary with I_0 in the same way as ν_{ei} versus I_0 since $\alpha \propto \nu_{ei}$. However, in some experiments [2,35], with normally incident s-polarized laser light, α was found to increase with I_0 up to a maximum value corresponding to an intensity I_c, and a decrease when $I_0 > I_c$. We explained this anomalous increase of α versus I_0 recently [29] with a variant of CSM [23–25] (called ballistic model, BM) using total velocity $v = \sqrt{v_0^2 + v_{th}^2}$ dependent $b_{max} = v/\omega$, and $b_{min} = Z/v^2$ in $\ln\Lambda$. However, all CSMs using $\ln\Lambda$ have deficiencies and do not always match with the more accurate kinetic models [22,26,32–34,36–39]) of ν_{ei} having no $\ln\Lambda$ dependence. Note that in kinetic models the upper cutoff b_{max} does not appear, and the only cutoff $k_{max} = 1/b_{min}$ is used. Naturally, the artifact introduced in $\ln\Lambda$ through b_{max} is questionable for CSMs. In fact, a large (unphysical) value of ν_{ei} may result with the CSM compared to the kinetic models (particularly) in the low temperature regime of our interest. For example, as $T_e \to 0$ the collision frequency predicted by CSM becomes abnormally so high that it predicts 100% fractional absorption. Although we used CSM in Ref. [29] to show anomalous absorption, the classical formulation may not be valid in the

very low temperature (e.g., $T_e \lesssim 5$ eV) regime for the classical nondegenerate plasmas.

To overcome the above mentioned limitations of CSM, in this work we use kinetic models (both quantum and classical) and show that anomalous variation of ν_{ei} and α with I_0 are possible to explain in the regime of low temperature (<15 eV) and underdense densities for a given laser wavelength, provided k_{max} is chosen in some appropriate form. By choosing the conventional classical cutoff $k_{max} = v_{th}^2/Z$ (see Refs. [22,33]) or the quantum cutoff $k_{max} = 2v_{th}$, we first show the so far unnoticed (i) anomalous increase of ν_{ei} versus T_e for a given I_0. Then we propose a modified $k_{max} = v^2/Z$ (for the classical case) or $k_{max} = 2v$ (for the quantum case), which additionally depends on E_0 and ω, and show (ii) anomalous increase of ν_{ei} vs I_0 for a given $T_e < 15$ eV. The anomalous variation of ν_{ei} and corresponding α with I_0 (also with T_e) are found only in the low temperature and low intensity regime as in our earlier work [29] with CSM, but it was not explored before with the kinetic models. The proposed k_{max} in the kinetic model is used to explain experimental results of laser absorption in Ref. [35], where the low intensity growing part of the absorption curve was not explained.

We assume a preionized, underdense plasma illuminated by laser light of different peak intensities. The wavelength of the pulse is $\lambda \approx 66$ nm, as considered in Ref. [33]. The condition for linear resonance absorption $\omega = \omega_p$, which requires a p-polarized light, is not satisfied for this case. However, collisional absorption may continue in the underdense pedestal region until the p-polarized light travels to the critical density (it is the density $n_c = \omega^2/4\pi$, where $\omega_p = \omega$ is met; for 66 nm, $n_c \approx 2.52 \times 10^{23}$ cm^{-3}) surface for the resonance absorption. Collisional absorption, as reported here, is independent of the polarization state of light, i.e., valid for s-polarized light also.

In Sec. II a description of kinetic models of ν_{ei} is given. Results of conventional and anomalous variation of ν_{ei} with T_e and I_0 are shown in Sec. III, and corresponding fractional absorption α vs I_0 is shown in Sec. IV with comparison to experiments. A summary of the work is given in Sec. V.

II. KINETIC MODELS OF ν_{ei}

Electron-ion collision frequency is related to the rate of laser energy absorption (in unit volume) $\dot{\epsilon} = \langle e n_e \boldsymbol{v_e} \cdot \boldsymbol{E} \rangle$ as

$$\nu_{ei} = 4\pi \left(\omega^2/\omega_p^2\right) \dot{\epsilon}/\langle \boldsymbol{E}^2 \rangle, \tag{1}$$

where v_e is the electron velocity. Depending upon $\dot{\epsilon}$ (either quantum mechanical or classical), we get ν_{ei} varying with $I_0 = E_0^2$. Assuming the Maxwellian velocity distribution for electrons (and stationary ions), the quantum mechanical expression [33] of $\dot{\epsilon}$ is given by

$$\begin{aligned}\dot{\epsilon} = {} & \frac{8\sqrt{2\pi} Z^2 n_e n_i}{v_e^3} \omega^2 \sum_{n=1}^{\infty} n^2 \int_{k=0}^{\infty} \frac{dk}{k^3 |\epsilon_{RPA}(k,n\omega)|^2} \\ & \times \exp\left[-\frac{1}{2}\left(\frac{n\omega}{k v_e}\right)^2 - \frac{1}{2}\left(\frac{k}{k_B}\right)^2 \right] \frac{\sinh(n\omega/k_B v_e)}{(n\omega/k_B v_e)} \\ & \times \int_0^1 J_n^2(k r_0 z)\, dz. \end{aligned} \tag{2}$$

Here $\epsilon_{RPA}(k,n\omega)$ is the quantum mechanical dielectric function (which is a complex quantity in general) in the random phase [26,33,40] approximation (RPA) due to Lindhard [41], $k_B = 2v_e/\hbar$ (note $\hbar = 1$ in a.u.) is the inverse of the DeBroglie wavelength λ_B, n is the order of the Bessel function $J_n(\mu)$, $r_0 = E_0/\omega^2$ is the excursion of a free electron in the laser field, and k signifies the inverse of the distance of the electron from the colliding ion. The summation over n indicates the contribution from different multiphoton absorption processes, with $n = 1$ being the single photon contribution to the absorption. The quantum effect enters through k_B. The integrals and the summation [in Eq. (2)] can be computed numerically with chosen upper limits of $n = n_{max}$ and $k = k_{max}$. The choice of k_{max} is crucial for ν_{ei}, and conventionally it is taken as $k_{max} = 1/b_{min} = v_{th}^2/Z$ [22,33]. Note that Eq. (2) is free from the cutoff $b_{max} = 1/k_{min}$, which is required for $\ln\Lambda$ in the case of CSM. The complex dielectric function $\epsilon_{RPA}(k,\omega)$ can be obtained from the relation [40]

$$\epsilon_{RPA}(k,\omega) = 1 + \frac{1}{2}\left(\frac{\omega_p}{k v_e}\right)^2 \frac{f(x - q/2) - f(x + q/2)}{q}, \tag{3}$$

where $f(x) = \pi^{-1/2} \int_{-\infty}^{\infty} dt \exp(-t^2)/(t - x)$ is the plasma dispersion function, $x = \omega/\sqrt{2} k v_e$, and $q/2 = k/\sqrt{2} k_B$. $f(x)$ is related to the the Dawson's integral $D(x) = \exp(-x^2) \int_0^x dt \exp(t^2)$ as $f(x) = -2D(x) + i\sqrt{\pi}\exp(-x^2)$. Detail calculation of $\epsilon_{RPA} = \epsilon_1 + i\epsilon_2$ leads to writing the real and imaginary parts as

$$\epsilon_1(k,\omega) = 1 + \frac{1}{\sqrt{2}}\left(\frac{\omega_p}{\omega}\right)^2 \left(\frac{\omega}{k v_e}\right)^2 G_2(k,\omega), \tag{4a}$$

$$\epsilon_2(k,\omega) = \sqrt{\frac{\pi}{2}}\left(\frac{\omega_p}{\omega}\right)^2 \left(\frac{\omega}{k v_e}\right)^3 G_1(k,\omega), \tag{4b}$$

where $G_1(k,\omega) = \exp\{-[(\omega/k v_e)^2 + (k/k_B)^2]/2\} \frac{\sinh(\omega/k_B v_e)}{(\omega/k_B v_e)}$, $G_2(k,\omega) = (k_B/k)[D_+(k,\omega) - D_-(k,\omega)]$, and $D_\pm(k,\omega) = D([\omega/k v_e \pm k/k_B]/\sqrt{2})$.

A. Classical approximation

Classical results of G_1, G_2, ϵ_1, and ϵ_2 can be obtained by setting $k_B \to \infty$ (for $\hbar \to 0$) giving $G_1^{CL}(k,\omega) = \exp[-\frac{(\omega/k v_e)^2}{2}]$, $G_2^{CL}(k,\omega) = \sqrt{2}[1 - \sqrt{2}(\frac{\omega}{k v_e}) D(\frac{\omega}{\sqrt{2} k v_e})]$,

$$\epsilon_1^{CL}(k,\omega) = 1 + \frac{1}{\sqrt{2}}\left(\frac{\omega_p}{\omega}\right)^2 \left(\frac{\omega}{k v_e}\right)^2 G_2^{CL}(k,\omega), \tag{5a}$$

$$\epsilon_2^{CL}(k,\omega) = \sqrt{\frac{\pi}{2}}\left(\frac{\omega_p}{\omega}\right)^2 \left(\frac{\omega}{k v_e}\right)^3 G_1^{CL}(k,\omega). \tag{5b}$$

To evaluate above limiting values, we have used the L'Hospital rule, antisymmetry, and derivative properties of $D(x)$, namely, $D(-x) = -D(x)$ and $D'(x) = 1 - 2xD(x)$, when required. Corresponding classical dielectric function $\epsilon_{RPA}^{CL} = \epsilon_1^{CL} + i\epsilon_2^{CL}$ gives the classical expression of energy absorption

rate,

$$\dot{\epsilon}^{\rm CL} = \frac{8\sqrt{2\pi}Z^2 n_e n_i}{v_e^3}\omega^2 \sum_{n=1}^{\infty} n^2 \int_{k=0}^{\infty} \frac{dk}{k^3 \left|\epsilon^{\rm CL}_{\rm RPA}(k,n\omega)\right|^2} \times \exp[-(n\omega/kv_e)^2/2] \int_0^1 J_n^2(kr_0 z)\, dz. \quad (6)$$

The Dawson-Oberman model (Eq. (22) in Ref. [22]) of ν_{ei} can be recovered from Eq. (6) by assuming $|\epsilon^{\rm CL}_{\rm RPA}|^2 \approx 1$, leading to

$$\dot{\epsilon}^{\rm CL}_{\rm Dawson} = \frac{8\sqrt{2\pi}Z^2 n_e n_i}{v_e^3}\omega^2 \sum_{n=1}^{\infty} n^2 \int_{k=0}^{\infty} \frac{dk}{k^3} \times \exp[-(n\omega/kv_e)^2/2] \int_0^1 J_n^2(kr_0 z)\, dz. \quad (7)$$

We use Eqs. (2), (6), (7) and obtain corresponding ν_{ei} from Eq. (1) for a given set of laser and plasma parameters. The CSM (called ballistic model, BM) of ν_{ei} given by Mulser *et al.* [25] is not described here for conciseness, but it will be used for comparison with the kinetic models whenever it is needed.

III. RESULTS FOR ν_{ei}

We now present results of ν_{ei} at various values of T_e considering different models mentioned above. Special attention is given to the low temperature regime. Plasma is assumed to be uniformly charged with $Z = 1$ (hydrogenlike), density $n_e = Zn_i = n_p = 10^{28}/m^3$, temperature $T_e = 25.86$ eV, and $\omega/\omega_p = 5$, giving the laser wavelength $\lambda \approx 66$ nm as considered in Ref. [33]. For numerical calculations of ν_{ei} we have chosen $n_{max} = 20$, and k_{max} is discretized up to $m_{max} = 100$ distinct values such that $k_{max} = m_{max}\,\Delta k$ and $k = m\,\Delta k$. The above parameters are kept unchanged unless mentioned explicitly.

A. Conventional variation of frequency

Figure 1 shows normalized frequency ν_{ei}/ω_p versus normalized velocity v_0/v_{th} using expressions (2), (6), (7) and the CSM [25,29] represented by "Bornath-Q," "Bornath-C," "Dawson-C," and "Mulser-C," respectively, for $T_e = 25.86$ eV. Results are plotted in log-linear [Fig. 1(a)] and log-log [Fig. 1(b)] scale for the purpose of comparison with Ref. [33]. In this case, we have used the conventional $k_{max} = v_{th}^2/Z$, and $b_{max} = v_{th}/\omega$ (b_{max} is used only for the CSM case with $\ln\Lambda$ shown as "Mulser-C"). The log-log plot [Fig. 1(b)] shows good agreement with Ref. [33] (see Fig. 1 of Ref. [33]), but the difference between different approximations of ν_{ei}/ω_p is not clear, which is more visible in Fig. 1(a). For $v_0/v_{th} > 1$, the quantum result ("Bornath-Q") is found to match very well with classical kinetic approximations ("Bornath-C" and "Dawson-C"), but it is a little overestimated for $v_0/v_{th} < 1$ by the classical kinetic approximations. Good agreement between the classical approximations ("Bornath-C" and "Dawson-C") for all values of v_0/v_{th} justifies the assumption $|\epsilon^{\rm CL}_{\rm RPA}|^2 \approx 1$ in Ref. [22]. The CSM ("Mulser-C"), however, shows relatively larger deviation (which is found to increase further for lower temperatures $T_e < 25.86$ eV) from the quantum result. This is due to the artificial cutoff b_{max} in the CSM ("Mulser-C"), suggesting that an improvement in $\ln\Lambda$ is required. Due to this deficiency, CSM is not pursued for further comparison. However, in all cases, the universally accepted, conventional feature is that ν_{ei}/ω_p remains almost constant up to a value of $v_0/v_{th} \approx 1$, and then it drops rapidly when $v_0/v_{th} \gtrsim 1$.

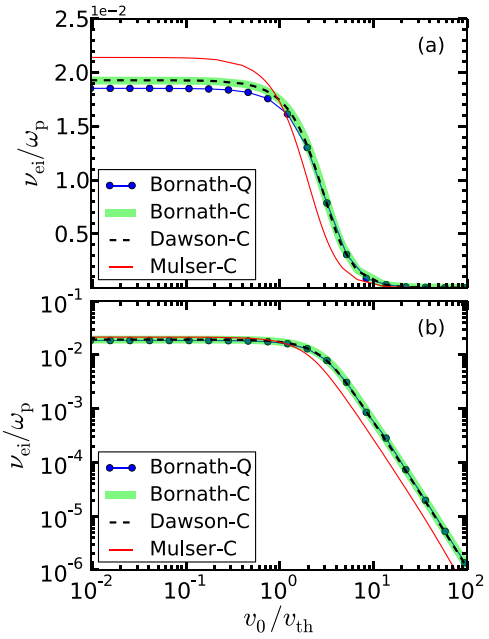

FIG. 1. (Color online) Variation of ν_{ei}/ω_p with v_0/v_{th} in (a) log-linear and (b) log-log scale with $T_e = 25.86$ eV, $Z = 1$, $n_p = 10^{28}/m^3$, and $\omega/\omega_p = 5$, giving $\lambda \approx 66$ nm. Legends describe different expressions used for ν_{ei}, e.g., "Bornath-Q" [Eq. (2)], "Bornath-C" [Eq. (6)], "Dawson-C" [Eq. (7)], and the ballistic model [25] by "Mulser-C," where we use $b_{min} = 1/k_{max} = Z/v_{th}^2$, $b_{max} = v_{th}/\omega$ for $\ln\Lambda$.

B. Anomalous variation of frequency

Unfortunately, collision frequency at a lower temperature $T_e < 25.86$ eV has not been studied in detail with kinetic models. From the literature [1,2] (and references therein) it is often unambiguously quoted that ν_{ei} should decrease with T_e as $\nu_{ei} \propto T_e^{-3/2}$. We show that this conventional conjecture is violated in the low temperature regime where ν_{ei} may increase with increasing T_e, *even* if the conventional cutoff $k_{max} = v_{th}^2/Z$ is taken to be true.

Figure 2 shows ν_{ei}/ω_p versus v_0/v_{th}, as in Fig. 1, with $T_e = 10$ eV [Fig. 2(a)] and $T_e = 15$ eV [Fig. 2(b)]. Apart from the common features, the comparison among Figs. 2(a), 2(b), and 1(b) clearly shows that ν_{ei}/ω_p increases from a value $\approx 2 \times 10^{-4}$ to $\approx 2 \times 10^{-2}$ (almost 100-fold increment) for $v_0/v_{th} < 1$ as T_e is increased from 10 to 25.86 eV. To show it more clearly, Fig. 3 depicts ν_{ei}/ω_p versus T_e for a fixed intensity $\sim 10^{14}$ W cm^{-2}. It shows that ν_{ei}/ω_p increases monotonically with increasing T_e up to a maximum value about $T_e \approx 35$ eV (indicated by a shaded region), and then ν_{ei}/ω_p decreases as T_e is increased beyond $T_e \approx 35$ eV. Just after the maximum the rate of decrease of ν_{ei}/ω_p is much slower (ν_{ei}/ω_p vs T_e is nearly linear up to ≈ 60 eV) than the conventional $\nu_{ei}/\omega_p \propto T_e^{-3/2}$ fall, shown by a thin dashed line.

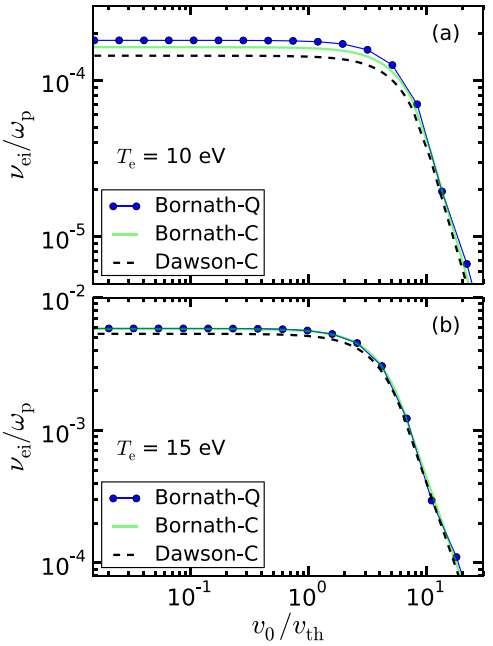

FIG. 2. (Color online) Variation of ν_{ei}/ω_p with v_0/v_{th} for (a) T_e = 10 eV and (b) T_e = 15 eV, using $k_{max} = v_{th}^2/Z$. Other parameters are the same as in Fig. 1.

1. *The effect of laser field*

So far, the effect of laser field strength has not been taken into account in k_{max} (in earlier kinetic models), which is not justified. k_{max} should depend on the parameters of the laser field through the ponderomotive velocity v_0 in some form which is not exactly known, and the conventional relation $k_{max} = v_{th}^2/Z$, as used previously, should be modified [25,29] depending on the total velocity $v = \sqrt{v_0^2 + v_{th}^2}$ of the electron. Replacing v_{th} with v in k_{max} and taking $k_{max} = v^2/Z$, we show below that

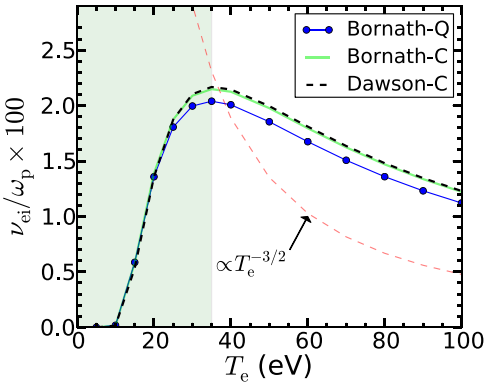

FIG. 3. (Color online) Variation of ν_{ei}/ω_p with T_e (in eV) using $k_{max} = v_{th}^2/Z$ and $I_0 = 10^{14}$ W cm^{-2}. Anomalous increase of ν_{ei}/ω_p is indicated by a shaded region. The $\nu_{ei}/\omega_p \propto T_e^{-3/2}$ line shows conventional scaling of ν_{ei}/ω_p with T_e, which does not obey kinetic results just after the frequency maximum with increasing T_e, but it may be valid for higher $T_e > 80$ eV, where the $T_e^{-3/2}$ line becomes parallel to the lines obtained by kinetic models. Other parameters are same as in Fig. 1.

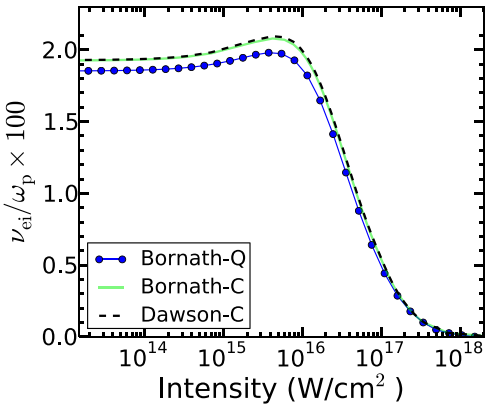

FIG. 4. (Color online) Variation of ν_{ei}/ω_p with the peak intensity for different kinetic models using total velocity dependent $k_{max} = v^2/Z$. Other parameters are same as in Fig. 1. Frequency increases up to a maximum value; after that, it decreases as the intensity is increased.

the conventional $I_0^{-3/2}$ decrease of ν_{ei} is also not obeyed in the low temperature and low intensity regime.

Figure 4 shows ν_{ei}/ω_p versus I_0 for the same parameters of Fig. 1, except that $k_{max} = v^2/Z$ has been used here. We have plotted ν_{ei}/ω_p against the peak intensity (instead of v_0/v_{th} as in Fig. 1) since it is an experimentally measurable parameter. For a fixed T_e = 25.86 eV (as in Fig. 1), ν_{ei}/ω_p [corresponding to Eqs. (2), (6), (7)] slowly increases with I_0 up to a maximum value. This anomalous increase of ν_{ei}/ω_p with I_0 (similar to ν_{ei}/ω_p versus T_e in Fig. 3) is due to the total velocity dependent k_{max} in the kinetic models, and it will be shown to be more prominent at a lower temperature in Sec. IV.

2. *Explanation for the anomalous increase of* ν_{ei}

To understand the anomalous increase of ν_{ei} with T_e and I_0 in the existing models, let us consider only the quantum case ("Bornath-Q") of Fig. 4. Here we restrict to smaller values of $n_{max} = 1$ and $m_{max} = 21$, with $k_{max} = v^2/Z$. For a chosen value of m where $1 < m \leqslant m_{max}$, the k integral is computed up to $m\Delta k$. Results are shown in Fig. 5 for successive values

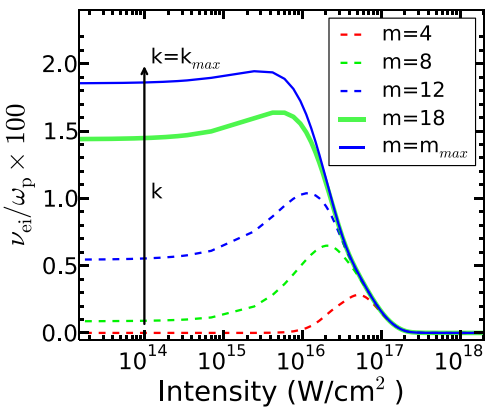

FIG. 5. (Color online) Variation of ν_{ei}/ω_p with intensity (using full quantum calculation, represented by "Bornath-Q" in Fig. 4) for successive k values up to k_{max} (represented by m up to m_{max}) and $n_{max} = 1$. Other parameters are the same as in Fig. 4.

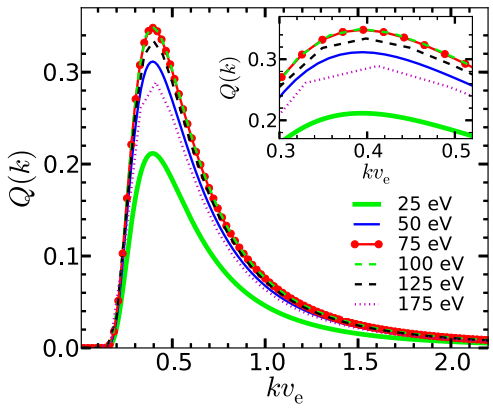

FIG. 6. (Color online) $Q(k)$ versus k (multiplied by $v_e = v_{th} = \sqrt{T_e}$) for $T_e = 25,50,\ldots,175$ eV with a fixed intensity 10^{14} W cm^{-2}. We have chosen $k_{max} = v_{th}^2/Z$, $m_{max} = 21$, and $n_{max} = 1$. Other parameters are the same as in Fig. 4. With increasing T_e the peak value of Q, and the area under the corresponding Q versus k, gradually increases to maximum value for $T_e = 75$–100 eV; then it drops for higher $T_e > 100$ eV.

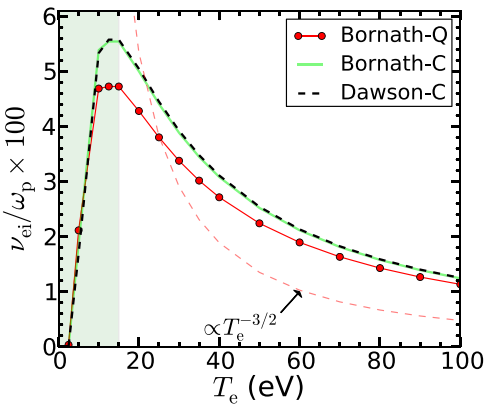

FIG. 7. (Color online) Variation of ν_{ei}/ω_p with T_e (in eV) using $k_{max} = 2v_{th}$. Anomalous increase of ν_{ei}/ω_p is indicated by a shaded region. The conventional scaling $\nu_{ei}/\omega_p \propto T_e^{-3/2}$ line does not obey kinetic results just after the frequency maximum with increasing T_e, but it seems to be valid for higher $T_e > 60$ eV, where the $T_e^{-3/2}$ line becomes parallel to the lines obtained by kinetic models. Other parameters are the same as in Fig. 1.

of k up to k_{max}. When k is small (for small m), frequency versus intensity variation shows a well defined peak which subsequently disappears when k increases to a higher value. It hints that anomalous increase in the frequency with intensity can be profound in the low temperature regime. The final curve for $k = k_{max}$ ($m = m_{max} = 21$) closely matches the quantum result in Fig. 4 ("Bornath-Q") for all intensities with less than 1% disagreement, although smaller values of m_{max} and n_{max} are chosen for Fig. 5. The present result with $n_{max} = 1$ indicates single photon absorption is the most dominant process, and the contributions from higher order photoabsorption processes with $n_{max} > 1$ are not so significant.

The minor difference between the quantum result ("Bornath-Q") and classical results ("Dawson-C" and "Bornath-C") in Figs. 3 and 4 suggests that the role of the terms $|\epsilon_{RPA}(k,n\omega)|^2$, $\exp[-(k/k_B)^2/2]$, and $\sinh(n\omega/k_B v_e)/(n\omega/k_B v_e)$ can be ignored at least for the understanding of the anomalous increase of ν_{ei} with T_e. Suppressing the prefactor, we express the remaining part of ν_{ei} [using Eqs. (1) and (2)] as

$$R = \frac{1}{I_0}\sum_{1}^{n_{max}}\int_0^{k_{max}} dk \left(\frac{n^2\omega^2}{k^3 v_e^3}\right)\exp\left[-\frac{1}{2}\left(\frac{n\omega}{k v_e}\right)^2\right] \times \int_0^1 J_n^2(kr_0 z)\,dz. \quad (8)$$

Since single-photon absorption is the dominant process, it will be sufficient if we understand the anomalous increase of ν_{ei} with respect to T_e for $n_{max} = 1$. In this case we write $R = I_0^{-1}\int_0^{k_{max}} dk\, Q(k)$, where the integrand $Q(k)$ reads

$$Q(k) = \left(\omega^2/k^3 v_e^3\right)\exp[-(\omega/k v_e)^2/2]\int_0^1 J_1^2(kr_0 z)\,dz. \quad (9)$$

Let us now keep I_0 fixed and vary T_e as in Fig. 3 with $k_{max} = v_{th}^2/Z$. In Fig. 6, we plot the function Q versus k (multiplied by $v_e = v_{th} = \sqrt{T_e}$) for $T_e = 25,50,\ldots,175$ eV. As T_e increases, the area under Q versus k curve first increases, reaches a maximum value for $T_e = 75$–100 eV (where curves are overlapped), and then it decreases for higher $T_e > 100$ eV (visible in the inset plot). The increasing area under the successive Q versus k curves with increasing T_e explains the anomalous growth of ν_{ei}/ω_p in Fig. 3 in the low temperature regime.

3. *Frequency variation with quantum cutoff*

In previous sections, we considered either a thermal velocity dependent cutoff $k_{max} = v_{th}^2/Z$ or a total velocity dependent cutoff $k_{max} = v^2/Z$. There may be a situation [33], where DeBroglie wavelength λ_B and the corresponding cutoff $k_B = 1/\lambda_B$ becomes important. For the sake of completeness, we now consider $k_{max} = k_B$. Traditionally, in the literature, only the thermal DeBroglie wavelength [33] leading to $k_{max} = k_B = 2v_{th}$ (in a.u.) is considered. Figure 7 shows ν_{ei}/ω_p vs T_e with the cutoff $k_{max} = 2v_{th}$ for the same parameters of Fig. 1. Initially, ν_{ei} increases with increasing T_e, reaches a maximum value, then drops as $T_e^{-3/2}$ for large T_e as in Fig. 3 where classical cutoff $k_{max} = v_{th}^2/Z$ was used. Compared to Fig. 3, the maximum value of ν_{ei}/ω_p is now higher, but the peak position is shifted toward a lower $T_e \approx 15$ eV, which is expected due to linear dependence of k_{max} on $v_{th} = \sqrt{T_e}$ in the present case. With two different cutoffs, we thus show anomalous increase in ν_{ei} in the low temperature regime.

The traditional quantum cutoff $k_{max} = 2v_{th}$, however, does not depend on laser field parameters and may not be justified when electrons are driven by the laser field. In Sec. IV we propose to use $k_{max} = k_B = 2v$ depending upon the total velocity v (as in Sec. III B 1) to study absorption of laser light in underdense plasma.

IV. COLLISIONAL ABSORPTION OF LIGHT WAVES IN UNDERDENSE PLASMA

We have shown that anomalous increase of collision frequency with temperature or intensity occurs in the low temperature and low intensity regime. This information can be

used to find absorption of laser light in an underdense plasma slab. In this case, the fractional absorption of light (at a normal incidence) can be written as [1,2]

$$\alpha = 1 - I_t/I_{inc} = 1 - \exp(-2\kappa_i L), \tag{10}$$

where I_{inc}, I_t are the incident and the transmitted intensity of light, $\kappa_i = (n/n_c)\nu_{ei}/v_g$, $v_g = c\sqrt{1-n/n_c}$ is the group velocity of light, and L is the thickness of the plasma slab. The relation $\alpha \approx 2(n/n_c)\nu_{ei}/v_g$ holds when κ_i is very small, and it shows that α should vary similarly to ν_{ei} with respect to T_e and I_0 for a fixed density of the plasma and laser frequency.

For illustration we assume a preionized plasma slab with density $n_p = n_c/25$ (i.e., $n_p = 10^{28}/m^3$) and thickness $L = 200\,\lambda$ irradiated by laser of wavelength $\lambda \approx 66$ nm. From Figs. 3 and 7 it is clear that anomalous frequency increase is possible if T_e is less than the value at which respective frequency maximum occurs. With the quantum cutoff $k_{max} = 2v_{th}$, the frequency maximum is shifted toward a lower value of T_e relative to the value corresponding to the classical cutoff $k_{max} = v_{th}^2/Z$ in Fig. 3. It means that if we intend to have frequency increase for both the cutoffs, then T_e should be well below 15 eV, which is evident from Fig. 7.

Figure 8 shows variation of ν_{ei}/ω_p, and corresponding α against I_0 using (i) $T_e = 15$ eV with the classical cutoff $k_{max} = v^2/Z$ [in panels (a) and (b)] and (ii) $T_e = 5$ eV with the quantum cutoff $k_{max} = 2v$ [in panels (c) and (d)]. Note that in both cases we have used total velocity dependent cutoffs. It is seen that ν_{ei} and α grow hand in hand up to a maximum value with increasing intensity up to $\approx 10^{16}$ W cm^{-2} (with the classical cutoff) and $\approx 5 \times 10^{15}$ W cm^{-2} (with the quantum cutoff), and after that they fall together. This anomalous growth of α was found in some experiments [2,35]. Earlier we provided an explanation [29] for this experimentally observed fact with a CSM [23–25] using total velocity dependent ln Λ. Here we find the same anomalous growing nature of α versus I_0 with more accurate kinetic models. It is seen that discrepancy persists among these models, which may be as large as 20% (for ν_{ei}) in the low intensity regime. When I_0 exceeds I_c, corresponding to the maximum of ν_{ei} (or α), discrepancy among different models tends to disappear.

Comparison with experimental results

Using the classical cutoff at $T_e = 15$ eV and the quantum cutoff at $T_e = 5$ eV, nearly 10%–35% and 30%–60% maximum absorption of light is predicted in Figs. 8(b) and 8(d), respectively (for the parameters considered here), at lower intensities $<5 \times 10^{15}$ W cm^{-2}. In Ref. [35] maximum fractional absorption was found nearly 65%, which is close to that in Fig. 8(d). Since $\nu_{ei} \propto n_p$, one can expect a higher value of α (either due to a higher $n_p < n_c$ or due to a larger plasma thickness L), and α may saturate to unity for a wide range of laser intensity. Such a high level of nearly 100% collisional absorption was also reported in experiments [2].

One may argue that reported experimental results [2,35] are at different wavelengths ($\lambda = 800$ nm, and $\lambda = 268$ nm), and it is not justified to compare those results with Fig. 8 at $\lambda = 66$ nm. To answer this, we have retrieved the experimental data from Ref. [35] and plotted in Fig. 9 along with the results from different kinetic models for $\lambda = 268$ nm. A plasma density of $n_p = 0.3n_c$, temperature $T_e = 5$ eV, and slab thickness $L = 10\lambda$ are assumed, since these parameters are unknown to us. The Fermi energy $E_F = (\hbar^2/2m_e)(3\pi^2 n_p)^{2/3}$ of electrons for $n_p = 0.3n_c$ and the Fermi temperature $T_F = 2E_F/5$ being much less than $T_e = 5$ eV, plasma can be assumed to be nondegenerate. Corresponding electron coupling parameter $\Gamma_e = e^2/a_e T_e$ ($a_e = n_p^{-1/3}$ is the interparticle distance) is found to be ≈ 0.5. For such a coupling strength, which is closer to unity, the classical Dawson-Oberman model [Eq. (7)] will break [33]. However, Eqs. (2) and (6) by Bornath *et al.* are still applicable. Good agreement is found between the experimental data and theoretical predictions at various intensities (specially below 10^{16} W cm^{-2}) with a growth of α up to a maximum value $\approx 65\%$ about an intensity $I_c \approx 10^{15}$ W cm^{-2} and a gradual decrease after I_c. Theoretical predictions are found to deviate significantly from the experimental data at intensities

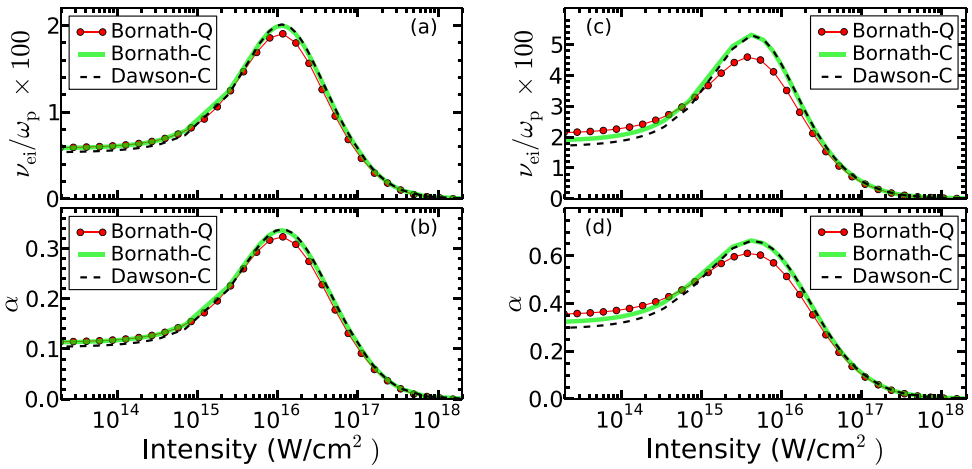

FIG. 8. (Color online) Variation of ν_{ei}/ω_p and α with laser intensity for a hydrogen like plasma of $Z = 1$, $n_p = 10^{28}/m^3$, and $n_p = n_c/25$. For (a), (b) $T_e = 15$ eV with classical cutoff $k_{max} = v^2/Z$, and for (c), (d) $T_e = 5$ eV with quantum cutoff $k_{max} = 2v$ are used. Thickness of the plasma slab is $L = 200\lambda = 13.38 \times 10^{-6}$ m.

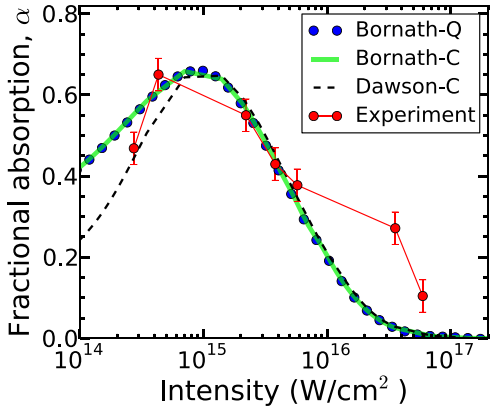

FIG. 9. (Color online) Comparison of experimental data (from Ref. [35]) of α versus I_0 with predictions from kinetic models for $\lambda = 268$ nm, $n_p = 0.3n_c$, $T_e = 5$ eV, and $k_{max} = v^2/Z$. Thickness of the plasma slab is chosen as $L = 10\lambda = 2.68 \times 10^{-6}$ m.

$>10^{16}$ W cm^{-2}. This may be due to the very simple assumption of a constant n_p. In reality, density modification is slow at lower intensities, but there may be significant rise in the plasma density when $I_0 > 10^{15}$ W cm^{-2}. Although there is no such rule which can self-consistently decide $n_p(I_0)$, we may assume a simple profile $n_p/n_c = 0.3\,[1 + 1.5\tanh(I_0/I_{a.u.})]$ as an illustration, where $I_{a.u.} = 3.51 \times 10^{16}$ W cm^{-2} is the intensity corresponding to 1 a.u. Results of α versus I_0 in Fig. 10 (with variable density) show an improved agreement of theoretical profiles with the experimental data, especially in the higher intensity side compared to that in Fig. 9. However, the modified, total velocity dependent k_{max} is not the only possibility which explains the experimental data well; there may be other unknown physical aspects for the anomalous nature of collisional absorption.

Anomalous behavior of absorption was also measured in Ref. [42] by offsetting the focal plane of the laser light with respect to the target front and in the laser-driven parylene disks [43]. However, physical explanation behind such absorption

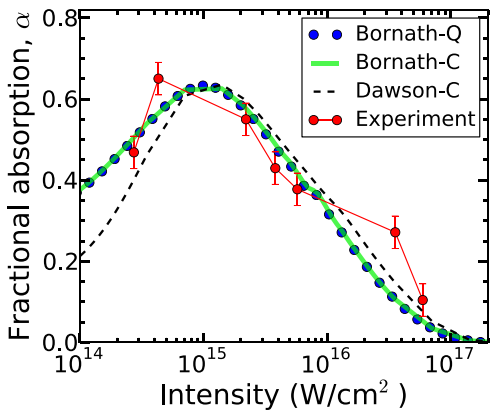

FIG. 10. (Color online) Comparison of experimental data (from Ref. [35]) of α versus I_0, with predictions from kinetic models, using a variable density profile $n_p/n_c = 0.3\,[1 + 1.5\tanh(I_0/I_{a.u.})]$. Other parameters are as in Fig. 9.

seems to be still lacking. In Ref. [42], possible reasons for anomalous absorption of light were thought to be due to "enhanced collisional absorption due to the ion turbulence or parametric decay instabilities" in a thin plasma layer adjacent to the critical density surface, and the resonance absorption process was not dominant. Experiments by Hass *et al.* [43] with a parylene disk target showed a gradual increase of fractional absorption from $\approx 27\%$ at $I_0 \approx 2 \times 10^{15}$ W cm^{-2} to $\approx 41\%$ at $I_0 \approx 4 \times 10^{16}$ W cm^{-2}, which is of "nonclassical" nature. The standard theory of collisional absorption cannot account for such anomalous absorption and deserves further investigation.

V. SUMMARY

We have reexamined electron-ion collision frequency ν_{ei} in an intense laser field and the corresponding absorption of laser pulses in an underdense plasma with existing quantum kinetic and classical kinetic models of ν_{ei}. Particular attention has been given to the low temperature ($T_e < 15$ eV) and low intensity ($I_0 < 5 \times 10^{14}$) regime where electron-ion collisions are significant. According to the conventional picture, most of the models [1,2,21,22,26,34,35] of ν_{ei} show that ν_{ei} (and the corresponding fractional absorption α) vary as $T_e^{-3/2}$ and $I_0^{-3/2}$ with respect to T_e and I_0, respectively. For a given intensity $I_0 < 5 \times 10^{14}$ W cm^{-2}, assuming the conventional expression of inverse cutoff distances $k_{max} = v_{th}^2/Z$ (classical) or $k_{max} = 2v_{th}$ (quantum) as used in the literature [22,33], it is shown that ν_{ei} increases monotonically to maximum as T_e is increased from a lower value and after the maximum ν_{ei} decreases according to the conventional relation $\nu_{ei} \propto T_e^{-3/2}$ when T_e is too high. Thus, the conventional picture is found to be true *only* in the high temperature and high intensity regime. Moreover, the conventional k_{max} only depends on the thermal velocity [22,33], which is not justified and must depend on the ponderomotive velocity $v_0 = E_0/\omega$. For a given $T_e < 15$ eV and a total velocity $v = \sqrt{v_{th}^2 + v_0^2}$ dependent k_{max} (proposed in this work), as the intensity is increased from a lower value $<5 \times 10^{15}$ W cm^{-2}, the frequency ν_{ei} is also found to increase monotonically up to a maximum value similar to ν_{ei} versus T_e at a constant I_0. The fractional absorption α which is almost proportional to ν_{ei}, follows the same anomalous variation with respect to T_e and I_0 as ν_{ei}. Thus, in both ways, we show growth of ν_{ei} and α with T_e and with I_0 up to a maximum using classical and quantum cutoff k_{max}. Anomalous increase of ν_{ei} with T_e and with I_0 were not pointed out earlier with kinetic models, because the low-temperature regime was not investigated as reported here.

Previously, we reported [29] similar anomalous increase of ν_{ei} (and α) by a CSM of ν_{ei} using a total velocity dependent Coulomb logarithm $\ln\Lambda(v)$ in the expression of ν_{ei}. However, the cutoff b_{max} used in $\ln\Lambda$ in CSM is a known artifact, and one may suspect that the anomalous increase of ν_{ei} and α in Ref. [29] were due to this effect. The kinetic models, however, are free from b_{max} and give qualitative support to our earlier findings [29]. Anomalous increase of fractional absorption with intensity was also observed in some experiments [2,35,43]. Our earlier work [29] using CSM and the present work using kinetic models with a

total velocity dependent k_{max} may be attributed to some of those experimentally [2,35,43] found anomalous collisional absorption. In fact, theoretical predictions are found to match well with the experimental results of Ref. [35].

ACKNOWLEDGMENTS

The author would like to thank Sudip Sengupta for fruitful suggestions and Richa Bandyopadhyay and Rajiv Goswami for careful reading of the manuscript.

[1] W. L. Kruer, *The Physics of Laser Plasma Interactions* (Addison-Wesley, New York, 1988).
[2] S. Eliezer, *The Interaction of High-Power Lasers with Plasmas* (IOP Publishing, Bristol, UK, 2002).
[3] P. Mulser and D. Bauer, *High Power Laser-Matter Interaction, STMP 238* (Springer, Berlin, Heidelberg, 2010).
[4] P. Gibbon, *Short Pulse Laser Interactions with Matter: An Introduction* (Imperial College Press, London, 2005).
[5] K. R. Manes, V. C. Rupert, J. M. Auerbach, P. Lee, and J. E. Swain, Phys. Rev. Lett. **39**, 281 (1977).
[6] P. Mulser and M. Kanapathipillai, Phys. Rev. A **71**, 063201 (2005).
[7] P. Mulser and M. Kanapathipillai, Phys. Rev. Lett. **95**, 103401 (2005).
[8] M. Kundu and D. Bauer, Phys. Rev. Lett. **96**, 123401 (2006).
[9] M. Kundu and D. Bauer, Phys. Rev. A **74**, 063202 (2006).
[10] M. Kundu, P. K. Kaw, and D. Bauer, Phys. Rev. A **85**, 023202 (2012).
[11] I. Kostyukov and J. M. Rax, Phys. Rev. E **67**, 066405 (2003).
[12] F. Brunel, Phys. Rev. Lett. **59**, 52 (1987).
[13] L. Schlessinger and J. Wright, Phys. Rev. A **20**, 1934 (1979).
[14] P. Hilse, M. Schlanges, Th. Bornath, and D. Kremp, Phys. Rev. E **71**, 056408 (2005).
[15] J. T. Mendonça, R. M. O. Galvão, A. Serbeto, S.-J. Liang, and L. K. Ang, Phys. Rev. E **87**, 063112 (2013).
[16] M. Moll, M. Schlanges, Th. Bornath, and V. P. Krainov, New J. Phys. **14**, 065010 (2012).
[17] G. J. Pert, J. Phys. A **5**, 506 (1972).
[18] G. J. Pert, J. Phys. B **8**, 3069 (1975).
[19] S. Rand, Phys. Rev. **136**, B231 (1964).
[20] S.-M. Weng, Z.-M. Sheng, and J. Zhang, Phys. Rev. E **80**, 056406 (2009).
[21] V. P. Silin, Zh. Éksp. Teor. Fiz. **47**, 2254 (1964) [Sov. Phys. JETP **20**, 1510 (1965)].
[22] C. D. Decker, W. B. Mori, J. M. Dawson, and T. Katsouleas, Phys. Plasmas **1**, 4043 (1994).
[23] P. Mulser and A. Saemann, Contrib. Plasma Phys. **37**, 211 (1997).
[24] P. Mulser and R. Schneider, J. Phys. A: Math. Theor. **42**, 214058 (2009).
[25] P. Mulser, F. Cornolti, E. Bésuelle, and R. Schneider, Phys. Rev. E **63**, 016406 (2000).
[26] H.-J. Kull and L. Plagne, Phys. Plasmas **8**, 5244 (2001).
[27] John Wesson, *Tokamaks* (Oxford University Press, Oxford, UK, 2004).
[28] G. J. Pert, Phys. Rev. E **51**, 4778 (1995).
[29] M. Kundu, Phys. Plasmas **21**, 013302 (2014).
[30] S. C. Rae and K. Burnett, Phys. Rev. A **46**, 2077 (1992).
[31] P. J. Catto and Th. Speziale, Phys. Fluids **20**, 167 (1977).
[32] D. Kremp, Th. Bornath, P. Hilse, H. Haberland, M. Schlanges, and M. Bonitz, Contrib. Plasma Phys. **41**, 259 (2001).
[33] Th. Bornath, M. Schlanges, P. Hilse, and D. Kremp, Phys. Rev. E **64**, 026414 (2001).
[34] A. Brantov, W. Rozmus, R. Sydora, C. E. Capjack, V. Yu. Bychenkov *et al.*, Phys. Plasmas **10**, 3385 (2003).
[35] D. Riley, L. A. Gizzi, A. J. Mackinnon, S. M. Viana, and O. Willi, Phys. Rev. E **48**, 4855 (1993).
[36] J. Dawson and C. Oberman, Phys. Fluids **5**, 517 (1962).
[37] A. R. Salat and P. K. Kaw, Phys. Fluids **12**, 342 (1969).
[38] A. Das and P. Kaw, Phys. Plasmas **5**, 2533 (1998).
[39] S. H. Kim and H. E. Wilhelm, Phys. Fluids **25**, 668 (1982).
[40] A. V. Latyshev and A. A. Yushkanov, arXiv:1003.2531v1.
[41] J. Lindhard, Dan. Mat. Fys. Medd. **28**, 1 (1954).
[42] A. Perry, B. Luther-Davies, and R. Dragila, Phys. Rev. A **39**, 2565 (1989).
[43] R. A. Haas, W. C. Mead, W. L. Kruer, D. W. Phillion, H. N. Kornblum, J. D. Lindl, D. MacQuigg, V. C. Rupert, and K. G. Tirsell, Phys. Fluids **20**, 322 (1977).